A domesticated fungal cultivar recycles its cytoplasmic contents as nutritional rewards for its leafcutter ant farmers

Caio Ambrosio Leal-Dutra[1*], Lok Man Yuen[2], Pedro Elias Marques,[3] Bruno Augusto Maciel Guedes[4], Marta Contreras-Serrano[1], Jonathan Zvi Shik[1,5]

[1] Section for Ecology and Evolution, Department of Biology, University of Copenhagen, Universitetsparken 15, 2100 Copenhagen, Denmark

[2] Department of Life Sciences, Imperial College London, London SW7 2AZ, UK

[3] Laboratory of Molecular Immunology, Department of Microbiology, Immunology and Transplantation, Rega Institute, KU Leuven, Leuven, Belgium

[4] Departamento de Ciências Básicas da Vida - Universidade Federal de Juiz de Fora, Campus Governador Valadares, MG, 35020-360, Brasil

[5] Smithsonian Tropical Research Institute, Apartado 0843-03092, Balboa, Ancon, Republic of Panama

* caio@bio.ku.dk

Authors email in order:

lok.yuen19@imperial.ac.uk

pedro.marques@kuleuven.be

bruno.guedes@ufjf.edu.br

contrerasserranomarta@gmail.com

jonathan.shik@bio.ku.dk

Competing Interests

The authors declare no competing interest.

Keywords: autophagy, *Leucoagaricus gongylophorus*, leafcutter ant, gongylidia, fungus, attini, attines

ABSTRACT

Leafcutter ants farm a fungal cultivar (*Leucoagaricus gongylophorus*) that converts inedible vegetation into food that sustains colonies with up to millions of workers. Analogous to edible fruits of crops domesticated by humans, *L. gongylophorus* has evolved specialized nutritional rewards—swollen hyphal cells called gongylidia that package metabolites ingested by ant farmers. Yet, little is known about how gongylidia form, and thus how fungal physiology and ant provisioning interact to farming performance. We explored the mechanisms governing gongylidium formation using microscopy imaging of ant-cultivated fungus and controlled *in vitro* experiments with the cultivar grown in isolation from ant farmers. First, *L. gongylophorus* is polykaryotic (up to 17 haploid nuclei/cell) and our results suggest intracellular nucleus distributions govern gongylidium morphology with their absence in expanding edges arresting apical growth and their presence mediating complex branching patterns. Second, nanoscale imaging (SEM, TEM) shows that the cultivar recycles its own cellular material (*e.g*. cytosol, mitochondria) through a process called 'autophagy' and stores the resulting metabolites in gongylidia. This autophagic pathway is further supported by gongylidium suppression when isolated fungal cultures are grown on media with autophagy inhibitors, and differential transcript expression (RNA-seq) analyses showing upregulation of multiple autophagy genes in gongylidia. We hypothesize that autophagic nutritional reward production is *the* ultimate cultivar service and reflects a higher-level organismality adaptation enabled by strict symmetric lifetime commitment between ant farmers and their fungal crop.

Introduction

The advent of domesticated agriculture some 10 000 years ago was a turning point for humans and for the domesticated crops whose derived traits would likely have been maladaptive in their free-living ancestors [1-3]. Key crop adaptations include whole genome duplication events (resulting in polyploidy) that can increase functional heterozygosity [4] and selection for specific regulatory genes that can reduce seed shattering or enhance fruit size, color, and sweetness [5-8]. Fascinatingly, humans are not the only farmers. Several insect lineages independently evolved obligate farming systems of fungal cultivars that produce specialized edible reward structures [9]. However, while human farmers modify growth environments in well-known ways to maximize crop yield (e.g. adding fertilizers, controlling watering conditions, etc.), the analogous mechanisms by which insect farmers promote expression of edible reward structures in fungal cultivars remain poorly understood.

The largest-scale insect farmers are the *Atta* leafcutter ants, the crown group of the fungus-farming 'attine' ant lineage [10, 11]. Despite clear analogies with farming systems of humans [9], farming by leafcutter ants is fundamentally different because it is 'organismal' in the sense that it represents a strictly symmetrical obligate mutualistic dependence [12]. Such an arrangement usually does not allow alternative crops, but does sustain selection for co-evolutionary integration and higher-level adaptation that cannot evolve when farming practices are asymmetrically promiscuous [13, 14]. These differences make it interesting to explore how leafcutter farmers regulate crop productivity, since they can help to: 1) understand the broad eco-evolutionary success of these naturally selected farming systems and 2) provide nutritional insights into whether the leafcutter ectosymbiosis has achieved an organismal level of conflict-free trait evolution typically only seen in lifetime committed endosymbioses (*e.g.* the mitochondria-nucleus partnership in eukaryotic cells [15, 16]).

A mature rainforest colony of the leafcutter ant *Atta colombica* can have millions of specialized ants that divide the work of foraging fresh plant fragments and caring for the fungal cultivar [17]. In this way, colonies convert foraged fragments from hundreds of plant species [18] into a mulch used to provision their fungal cultivar *Leucoagaricus gongylophorus*. In return, the cultivar converts inedible plant biomass into edible reward structures called gongylidia, that are swollen hyphal cells *ca.* 30 µm in diameter and grow in bundles called staphylae [19-27].

Gongylidia are a defining trait of irreversible crop domestication and are unique to the fungal lineage farmed by leafcutter ants and other higher-neoattine genera including *Trachymyrmex*, *Sericomyrmex*, *Mycetomoellerius*, and *Paratrachymyrmex* [20, 28, 29].

Gongylidia mediate functional integration with their ant symbionts in two main ways. First, they contain enzymes (*e.g.*, laccases, pectinases, proteases) that ants ingest and then vector to patches of newly deposited vegetation to catalyze fungus-mediated digestion and detoxification [30-34]. Second, they contain nutrients (*e.g.*, amino acids, lipids and glycogen) that are the ants' primary food source [35, 36]. The ability to regulate the quantity and quality of gongylidia would thus provide clear benefits for the ant farmers. However, the mechanisms linking substrate provisioning by farming ants and the production of the cultivar's edible yield have remained poorly known. To better understand these mechanisms, we: 1) visualized the morphology of gongylidia and staphylae using scanning electron microscopy (SEM), 2) described the cellular reorganizations that mediate gongylidium formation by combining light, fluorescence, confocal and transmission electron microscopy (TEM), and 3) used a transcriptomics experiment to compare gene expression in hyphae and gongylidia to help resolve the metabolic pathways underlying gongylidia production.

We next examined the cellular origins of the edible resources contained in the large vacuole that fills each gongylidium cell. Previous evidence suggests that *L. gongylophorus* directly metabolizes provisioned plant fragments to produce these edible resources. First, the cultivar can metabolize lipids rich in alpha-linoleic acid (18:3) from foraged plant fragments into linolenic acid (18:2) that is enriched in gongylidia [37]. This synthesized metabolite is thought to mediate interkingdom communication by eliciting attractive behaviors in ant workers, in contrast to the precursor 18:3 lipid that elicits antagonistic behaviors [37]. Second, isotopic enrichment studies have shown that the cultivar quickly (within two days) shunts C and N from provisioned substrates (glucose and ammonium nitrate, respectively) into edible gongylidia [38]. Third, different substrate types are associated with increased expression of genes regulating targeted pathways for nutritional metabolism [21, 36, 39, 40]. However, it is also reasonable to predict that the diversity of compounds found within gongylidia have a diversity of biochemical origins.

Autophagy is a plausible alternative and/or complementary pathway underlying gongylidia formation that involves the recycling of the cultivar's own metabolic source material

and potentially the fine-tuning of its composition. The metabolic pathways for autophagy are conserved across eukaryotes and are known to mediate development, cellular differentiation [41-44], and housekeeping [45, 46] in fungal cells. During autophagy, the cultivar's own cytoplasmic components (*i.e.*, glycogen, proteins, organelles) are incorporated into a vacuole for enzymatic degradation and the resulting catabolites are then recycled as nutrients to sustain other cellular processes and produce new cellular components [47, 48]. Initial evidence for autophagy in *L. gongylophorus* was first obtained in 1979 by Angeli-Papa and Eymé [49] who used TEM imaging to observe endoplasmic reticulum membranes engulfing mitochondria during gongylidium formation. However, to our knowledge, this preliminary evidence for autophagic recycling of the cultivar's own intracellular content during gongylidium formation has not been subsequently explored.

We propose that confirmation of an autophagic pathway(s) would have important implications for understanding the leafcutter symbiosis since it implies that natural selection has targeted the farming symbiosis in ways that made provisioning more robust and less dependent on the variable quality and quantity of foraged vegetation. Specifically, we predict that autophagic nutrient recycling of cellular contents would: 1) reduce variability in the quality of the cultivar's nutritional rewards and provide opportunities to optimize the composition of metabolic source material, 2) constrain the ability of ants to directly regulate cultivar productivity through their provisioning decisions, and 3) function in a complementary manner to provisioned plant substrates by providing a stable supply of metabolic precursor substrates during periods of environmental vegetation shortage.

We tested for autophagic gongylidium formation in three ways. First, autophagy encompasses two main types of cellular recycling mechanisms: 1) macroautophagy in which cytoplasmic content (i.e. cytosolic metabolites and organelles) are sequestered into double-membraned vesicles that fuse with vacuoles, and 2) microautophagy in which the vacuolar membrane invaginates and directly engulfs cytoplasmic cargo [47, 48]. We determined whether and how these autophagic processes influence gongylidium formation by examining organelle rearrangements in TEM images and tracking experimentally supplied fluorescent-labeled nutrients using confocal microscopy. Second, we tested whether autophagy is necessary for gongylidium formation by performing an *in vitro* experiment where the density of staphyla was

142 measured in cultivars grown with known inhibitors and promoters of autophagy in fungal cells.
143 Third, we tested whether autophagic pathways are differentially expressed in developing
144 gongylidium cells by performing transcriptomic analyses of the mycelia and differentiated
145 staphylae of the cultivar when grown under controlled *in vitro* conditions on a standardized
146 medium without ant farmers.

147

148 **Results**

149 ***Nutritional reward structures***

150 Each gongylidium cell consists of two sections that we term the bulb (swollen section)
151 and the filament (elongated section) (Fig. 1 A). Gongylidia are often connected by intercalary
152 bulbs (between filaments) and intercalary filaments (between bulbs) (Fig. 1 B-C) with
153 multifaceted branching patterns and individual gongylidium cells bearing two or more terminal
154 bulbs (Fig. 1 D). Gongylidia bulbs have variable diameters ranging from 12 µm to 50 µm and
155 variable filament lengths ranging from 40 µm to > 250 µm. We hypothesize that variable bulb
156 sizes reflect indeterminate growth trajectories of expanding gongylidium cells. All gongylidium
157 cells also contained at least eight nuclei usually concentrated at the intersection of the bulb and
158 the filament (Fig. 1 E) and usually one single vacuole (Fig. 1 F) that comprised up to half of
159 each bulb's total volume.

160 Individual staphylae range widely in size, with tens to hundreds of individual
161 gongylidium cells (Fig. 1 G, Fig. S1), and always formed on the surface of fungus garden
162 mycelial matrix where ants can easily detach them from surrounding hyphae. Staphylae also
163 form in the absence of ants under *in vitro* (Petri dish) growth conditions, but they have the
164 following key morphological differences compared to those growing in ant-tended fungus
165 gardens, being: 1) less detachable because they are usually covered by filamentous hyphae, 2)
166 larger in area and with more individual gongylidium cells, and 3) comprised of several 'burst'
167 gongylidium cells. We thus propose that under farming conditions, ants harvest staphylae
168 earlier in their development before vacuoles can produce turgor pressure exceeding the
169 retaining capacity of their exceptionally thin (ca. 120 to 220 nm) cell walls (Fig. 1 H).

170

An autophagic mechanism of gongylidia formation

Microscopy images (TEM, light, fluorescence and confocal) of gongylidium cells revealed structures that are diagnostic of macroautophagic processes. First, gongylidia were enriched with long stretches of endoplasmic reticulum that produce double-membraned vesicles called autophagosomes (Fig. 2), within which recycling of cellular materials is initiated. We confirm that autophagosomes contained cytosol (Fig. 2 A), glycogen (Fig. 2 B) and mitochondria (Fig. 2 C), and predict that other metabolites (*e.g.*, lipids, amino acids, enzymes [28, 30, 37, 40, 64]) are likely abundant, but are too small to be detected with TEM. Second, large numbers of damaged mitochondria were present in gongylidia and were often associated with endoplasmic reticulum membranes (Fig. 2 C) where they were likely destined to be sequestered into autophagosomes, digested, and recycled into edible metabolites. Third, vacuoles within gongylidium bulbs often contained single-membraned autophagic bodies (Fig. 2 D-F). These vesicles indicate the delivery of metabolites into vacuoles, since they are autophagosomes that lost their outer membrane after vacuolar fusion. This was confirmed by confocal images showing that autophagic bodies within gongylidium vacuoles contained fluorescently labeled sugars from the cultivar's cytosol (Fig. 2 E-F, Video S1). Given these hallmarks of macroautophagy (and the lack of evidence for microautophagy), we henceforth use 'autophagy' to refer to macroautophagy.

An autophagic mechanism for gongylidium formation was further supported by significant *in vitro* treatment effects of chemical autophagy inhibitors on staphyla density (Kruskal-Wallis: $H_3 = 34.7$, $p < 0.001$, Fig. 3). Pairwise post-hoc comparisons indicated that both autophagy inhibitors (3-MA and CQ) had significantly reduced staphyla density compared to both the control (PDA) ($p_{adj} < 0.001$ and $p_{adj} = 0.001$, respectively) and the autophagy-promoter (RAP) treatment ($p_{adj} < 0.001$ and $p_{adj} = 0.026$, respectively). There was also a significant treatment effect on mycelial growth area ($H_3 = 16.3$, $p = 0.001$). However, this was due to differences between 3-MA and all other treatments (PDA:3-MA, $p_{adj} = 0.004$; RAP:3-MA, $p_{adj} = 0.015$; CQ:3-MA, $p_{adj} = 0.001$), with no other significant pairwise comparisons (Fig. S2). Thus, while both autophagy inhibition treatments resulted in staphyla reduction, it is possible that 3-MA negatively influenced staphyla density through unknown indirect effects on cultivar

performance. The autophagy promotor (RAP) did not significantly increase staphyla density relative to control (PDA) or either of the autophagy inhibition treatments (Fig. 3).

Transcriptome assembly and autophagy pathway analysis

Using a *de-novo* assembly and a clustering analysis by similarity, we recovered 78,820 transcripts from the *L. gongylophorus* transcriptome of which, 4,755 were differentially expressed (log2 fold-change > 1.0, Benjamini–Hochberg adjusted $P < 0.001$) in staphylae (n = 3,011 transcripts) or in non-differentiated mycelia (n = 1,744 transcripts). Of these differentially expressed transcripts (DETs), 31 were assigned a KEGG orthology term associated with the yeast autophagy pathway (n = 22 in staphylae, n = 9 in mycelia, Table 1). Several key genes were upregulated in staphylae that are typically over-transcribed during autophagy [48]. These include genes (ATG7, ATG8, ATG10) linked to the recruitment of cargo into incipient unclosed membranes (*i.e.*, phagophores) and mature autophagosomes, as well as genes related to starvation signaling (Sch9, Tap42, ATG13 and RIM15), vacuole fusion machinery (Ypt7, Mon1 and Vps3), and degradation of autophagic bodies (PRB1 and ATG15) (Table 1, Fig. S3). In contrast, the few autophagy-specific genes upregulated in undifferentiated mycelia appear related to the starvation signaling step of autophagy induction, rather than a fully functioning autophagy pathway.

Discussion

Our results provide novel insights into the mechanisms of higher-level homeostatic integration in a uniquely 'organismal' insect-microbe ectosymbiosis. Several lines of evidence indicate that the fungal cultivar of leafcutter ants uses autophagic recycling to convert its own cellular material into edible metabolites within specialized nutritional reward structures. First, nanoscale imaging shows the cellular hallmarks of autophagy (*e.g.* autophagosomes, autophagic bodies, abundant endoplasmic reticula) and indicates rapid delivery of labeled cytosol nutrients into gongylidium vacuoles (ca. 30 minutes). Second, experimental suppression of autophagy suppresses gongylidium density. Third, we find an upregulated autophagy pathway associated with differentiated gongylidium cells. We hypothesize that this autophagic

recycling pathway represents a final domestication step where the cultivar came to unambiguously prioritize nutritional services to its hosts even at the expense (up to a point) of its own mycelial health. In this sense, the autophagic recycling pathway expresses an obligately symmetric commitment between symbionts achieved after the domesticated fungal cultivar lost the capacity for a free-living existence and became fully integrated into the host colony's germ line.

We further propose that autophagic recycling facilitates homeostasis at higher levels of organization by stabilizing the quantity and nutritional quality of the cultivar's nutritional rewards in fluctuating environments. First, the seasonal and spatial availability of preferred plant fragments may vary in suboptimal ways [65, 66]. Second, foraged plant fragments can contain key nutrients—but these nutrients can occur in suboptimal ratios and concentrations relative to the cultivar's intrinsic needs and tolerances [19]. Third, plant fragments contain a wealth of recalcitrant compounds (e.g. cellulose and lignin) and toxic metabolites that can reduce cultivar performance [67-70]. During such periods of plant-fragment shortage [71-73], the cultivar may use autophagic recycling of its own organelles to yield reliably available and chemically predictable metabolic precursor compounds. Analogous adaptations aimed solely regulating homeostasis at higher levels of organization are absent from all other ectosymbioses that are promiscuous by comparison, where the interests of symbionts are not completely aligned, and partners must screen, sanction, and police to dissuade cheating [74-76].

The discovery of autophagic recycling also provides a new lens to interpret well-known gardening behaviors in leafcutter ants. For instance, gardening ants constantly prune the cultivar's fungal mycelia and this has been hypothesized to cause mechanical disruptions that stimulate gongylidium formation [77]. We propose that such pruning behaviors sever hyphal connections and block the flow of nutrients to newly isolated fungal cells, which in turn induces gongylidium formation by causing an autophagic response to starvation—which is a common driver of autophagy in cells [50]. Additionally, previous *in vitro* studies have observed highest staphylae densities at the lowest nutrient concentrations suggesting a link between staphyla formation and nutrient depletion [19, 40, 78-80]. Thus, while much research assumes that cultivar production hinges on a maximized flow of provisioned plant fragments [19, 53, 81], the

behaviors linked to targeted nutritional suppression may also be important for the production of nutritional rewards.

While gongylidia-linked autophagic recycling appears common, it likely complements other nutritional reward production mechanisms. First, leafcutter ants frequently ingest gongylidia contents (crushing the gongylidia to ingest their cellular content) and vector the cultivar's enzymes [31, 32, 34, 35] and nutrients [35, 36] as fecal droplets to catalyze degradation and detoxification of newly deposited plant fragments [30]. Metabolites within these fecal droplets are assimilated by the cultivar and some subset likely enters biosynthetic pathways linked to gongylidium formation. Second, key nutrients also appear to derive from bacterial symbionts (rather than plant fragments or autophagic recycling) [82-84]. For instance, attine ants have lost the ability to synthesize arginine [80]—and depend on the cultivar's metabolism to produce this nitrogen-rich amino acid [28]. In turn, the ants have evolved tight mutualistic associations with specialized bacterial symbionts that convert excess arginine in the ants' guts into ammonia (the Mollicutes EntAcro1, [84]) that is an N-rich fertilizer vectored by the ants back to their fungal symbiont. As further evidence that the autophagic-recycling is one of several mechanisms by which gongylidia fill with metabolites, we observed that staphyla production was still possible (even though significantly reduced) when autophagy was inhibited in the *in vitro* experiment. Resolving whether and how these nutritional pathways fluctuate relative to the specific resource needs of the colony thus represents an important next step.

Reconstructing the cellular reorganizations enabling gongylidium formation

The combined evidence we present throughout this study enables us to propose a complete pathway for gongylidia development (Fig. 4). Tissue differentiation initiates when a hyphal cell growing at surface interstices within the fungus garden matrix widens (Fig. 4 A) and continues as a vacuole begins expanding in response to autophagic recycling. This process accelerates autophagosomes fuse with the vacuole and delivers cytoplasmic cargo (Fig. 4 B). The location of this vacuole shapes the morphology of developing gongylidia because it mediates the spatial distributions of the up to 17 [86] haploid nuclei within individual gongylidium cells by excluding them from the apical tip (Fig. 4 C).

We hypothesize that the obstruction of nuclear migration causes the bulb's balloon-like expansion by blocking communication between nuclei and the Spitzenkörper—the centralized machinery for hyphal growth located in the hyphae tip. At the transcript level, a structurally modified and upregulated transcript carrying a domain associated with microtubule related proteins [40] may mediate such nuclear migration in association with motor protein complexes [87-89]. This mechanism would resemble growth dynamics in most filamentous fungi where nuclei are distributed evenly throughout the hyphal compartment and promote tip elongation by migrating apically [88, 90]. Further supporting this hypothesis, when nuclei are occasionally aggregated in different regions of the filament and bulb, they are associated with ramified branching gongylidia and intercalary bulb formation. Finally, we propose that staphylae arise from this patchy ramification of tangled gongylidia (Fig. 4 D).

These results can also inform our understand of the functional consequences of polyploidy in the domesticated *L. gongylophorus* cultivar which contains up to 7 distinct haplotypes per cell [86]. Specifically, key next steps involve moving beyond distributions of nuclei in gongylidium cells, to testing whether factors like nucleus-specific expression and nuclear dominance are linked to gongylidium formation. Such a mechanism has recently been observed in the production of edible reward structures produced by the heterokaryon human-domesticated champignon fungus (*Agaricus bisporus*), where two distinct nuclear types exhibit differential expression in distinct tissues during mushroom formation [91]. The convergent existence of such molecular mechanisms in gongylidium formation would provide a further means of testing the hypothesis that these nutritional rewards are derived from cystidia [20], which are modified hypha found in the hymenium of several groups of basidiomycetes [92, 93]. Autophagic induction of cystidia may have provided crucial pre-adaptations harnessed by natural selection to generate the unique gongylidium reward structures.

Methods

Sample acquisition and fungal symbiont isolation

Two colonies of *Atta colombica* (Ac2012-1 and Ac2019-1) were used in this study that were collected in Soberanía National Park, Panama and thereafter maintained at the University

of Copenhagen in a climate-controlled room (25°C, 70% RH, minimal daylight). For microcopy and imaging, we used staphylae collected directly from the colonies' fungus gardens, and for the autophagy inhibition experiments and transcriptome sequencing, we used axenic cultures isolated from the fungal cultivar (*L. gongylophorus*) grown in 90 mm Petri dishes filled with 20 ml potato dextrose agar (PDA) that were kept in the dark at 25°C.

Imaging morphology of staphyla and gongylidia

Using samples collected directly from the fungus gardens of live leafcutter colonies, we first used scanning electron microscopy (SEM) to visualize the external morphology of gongylidia and staphylae. The samples were fixed in PBS with 0.1% Tween 20 and fixatives (4% glutaraldehyde, 4% formaldehyde) and then dehydrated in an ethanol series (35%, 55%, 75%, 85%, 95%, and 2x in 100%) for 30 minutes per concentration, critical-point dried, coated with platinum, and imaged on a JSM-840 scanning electron microscope (JEOL, Tokyo, Japan) at 7.0 kV at the Zoological Museum of the University of Copenhagen. A slight wrinkled appearance of the surface of gongylidium cells in the resulting SEM images was due to unavoidable plasmolysis caused by the preparation process.

We then used light, fluorescence and confocal microscopy to view the cultivar's internal morphology (*e.g*. septa, vacuoles, nuclei, etc.) and examine cellular reorganizations associated with gongylidium induction. For all imaging, staphylae were first placed in a drop of mounting solution (dH_2O, PBS, 3% KOH) on a glass slide. Gongylidia were then separated under a stereo microscope (16x or 25x magnification) with 0.16-mm diameter acupuncture needles and stained. For visualization with white light, we placed samples in either 0.1% Congo-red (in 150 mM NaCl) for one minute followed by a wash with 150 mM NaCl, or 1.5% phloxine followed by a wash with 3% KOH. For nucleus visualization under UV light, we stained samples for 10 minutes using "Vectashield with DAPI" (Vector Laboratories, Burlingame, CA, USA). For confocal imaging, we stained the staphylae with dextran conjugated with Alexa Fluor 647 (Invitrogen, MA, USA) in the concentration of 100 µg/ml in PBS for 30 minutes and washed twice in PBS. We then acquired images at magnifications of up to 400x by performing bright-field, dark-field, phase-contrast, and fluorescence microscopy under an Olympus BX63 microscope (Olympus, Tokyo, Japan). The microstructures were measured and photographed using a mounted QImaging Retiga 6000 monochrome camera and cellSens Dimension v1.18

(Olympus) image-processing software. Confocal images were acquired with a Dragonfly spinning-disk confocal system (Andor Technology, Belfast, Northern Ireland) equipped with a 25x water-immersion objective. Samples were excited with a 637 nm laser line and fluorescence was collected with a 698/77 emission filter. Images were processed using FIJI software.

We next used transmission electron microscopy (TEM) to visualize fungal cells with greater magnification and resolution (i.e. the 500 nm scale). Staphylae were collected from fragments of intact fungus gardens, fixed in 2% glutaraldehyde in 0.05 M PBS (pH 7.2) and then post-fixed in 1% w/v OsO_4 with 0.05M $K_3Fe(Cn)_6$ in 0.12 M sodium phosphate buffer (pH 7.2) for 2 hr at room temperature. Fixed samples were washed three times in ddH_2O for 10 minutes and dehydrated in a series of increasing ethanol concentrations series (70%, 96% and 99.9%). Each dehydration lasted 15 min and was performed twice per concentration. Samples were then repeatedly infiltrated for 20 to 40 min with increasing Resin Epon:Propylene oxide ratios (1:3, 1:1, 3:1) and subsequently embedded in 100% Epon and polymerized overnight at 60°C. Sections of 60 nm thickness were then cut with an Ultracut 7 ultramicrotome (Leica, Vienna, Austria), collected on copper grids with Formvar supporting membranes, and stained with both uranyl acetate and lead citrate. These samples were TEM imaged on a CM100 BioTWIN (Philips, Eindhoven, The Netherlands) at an accelerating voltage of 80 kV. Digital images were recorded with a side-mounted OSIS Veleta digital slow scan 2 × 2 k CCD camera and the ITEM software package (Olympus Soft Imaging Corp, Münster, Germany). This sample preparation and imaging was performed at the Core Facility for Integrated Microscopy at the University of Copenhagen.

Autophagy inhibition assay

We tested the role of autophagy in gongylidium production using an *in vitro* growth assay with four treatment groups. Autophagy is often initiated in cells when the target of rapamycin kinase (TOR) is inhibited. Autophagy can thus be induced *in vitro* by adding rapamycin (RAP) [50] an allosteric TOR inhibitor [48]. Autophagy is often inhibited *in vitro* using Chloroquine (CQ) or 3-methyladenine (3-MA), as these compounds respectively block

375 autophagosome-vacuole fusion [51] and suppress an enzyme (class III PtdIns3K) required to
376 initiate autophagosome formation [52]. We compared cultivars grown in the dark for 46 days at
377 25°C on a baseline Potato Dextrose Agar (PDA) medium containing nutrients known to
378 maximize cultivar performance [19, 53] (n = 40) with cultivars grown on plates with RAP (n =
379 27), CQ (n = 28), or 3-MA (n = 30). Briefly, 5-mm diameter fungus plugs from previously isolated
380 and reinoculated PDA culture were placed in 60-mm Petri dishes containing 10 ml of PDA
381 (control), PDA + 300 ng/ml rapamycin (Medchem Express, Monmouth Junction, NJ, USA), PDA
382 + 1.5 mM chloroquine diphosphate (Sigma-Aldrich, St. Louis, Missouri, USA), or PDA + 10 mM
383 3-MA (Medchem Express). We then photographed plates to measure growth area (mm^2) using
384 ImageJ [54] and directly counted the staphylae on these Petri dishes under a stereo microscope
385 (40x magnification) to quantify staphyla density (number of staphylae/growth area). The
386 measurement of growth area also enabled assessment of other unintended inhibitory effects of
387 the added chemicals on cultivar performance. We tested for treatment effects (PDA-Control,
388 RAP, CQ, 3-MA) on mycelial growth and staphyla density in R version 4.0.2 [55] using a
389 Kruskal-Wallis test in *rstatix* version 0.7.0 [56] with pairwise post-hoc tests performed using
390 Dunn's Test in *rstatix* with adjusted p-values calculated using the false-discovery rate method.

391

392 ***Transcriptome sequencing, assembly and differential expression analyses***

393 To detect whether upregulated transcripts in staphylae were enriched with autophagy
394 genes, we first collected staphylae and undifferentiated mycelia from axenic fungal cultures
395 isolated from an *A. colombica* colony (Ac2012-1) and grown on PDA medium for 30 days as
396 specified above. From individual Petri dishes, we then used a RNeasy plant mini kit (Qiagen,
397 Germany) to extract total RNA from differentiated staphyla (pooled 200 staphylae individually
398 collected with sterile acupuncture needles, n = 5 Petri dishes samples) and undifferentiated
399 mycelia (adjacent mycelia lacking staphylae, n = 5 Petri dishes samples). Samples were
400 immediately placed in Qiagen RLC buffer containing 10uM DTT and RNA was then extracted
401 using the manufacturer-specified protocol. These samples were sent to BGI Europe
402 (Copenhagen, Denmark) where mRNA enrichment with oligo dT and strand-specific libraries
403 were constructed using dUTP in the cDNA synthesis. For each sample, between 24 and 30

404 million clean 100bp paired-end reads were generated by a DNBseq-G400 sequencer (MGI
405 Tech, Shenzhen, China).

406 We used pooled clean reads from all samples (staphylae and mycelia) to assemble a *de*
407 *novo* transcriptome using Trinity-v2.12.0 [57] and default settings with the addition of Jaccard-
408 clip and strand-specific (SS) options, to reduce the generation of chimeric transcripts and
409 account for the SS library construction, respectively. All downstream tools accounted for SS
410 sequences (analyzing only positive strands or sequences). Using CD-HIT [58] to cluster highly
411 similar sequences (98% similarity), we reduced the assembly from 93,470 to 78,820 transcripts
412 ranging from 187 to 26,203 bp. We used Trinity built-in pipelines to first estimate transcript
413 abundance with RSEM v1.3.1 [59] and then build a transcript expression matrix. We then
414 performed a differential expression analysis with a trinity built-in pipeline using DESeq2 [60]
415 setting the analysis to filter for the differentially expressed transcripts (DETs) with $\log_2$ fold
416 change > 1.0 and $P < 0.001$. To annotate the DETs, we first converted transcripts to amino acid
417 sequences using Transdecoder (https://github.com/TransDecoder/TransDecoder) to identify the
418 longest open read frames (orfs) per transcript and translate them into amino acid sequences,
419 and then annotated the DETs with KEGG database [61] using the online tools BlastKOALA,
420 GhostKOALA [62] and KofamKOALA [63].

421

422 **Data availability**

423 All the generated RNA-seq datasets are available at NCBI under the BioProject ID
424 PRJNAXXXXXX.

425

426 **Acknowledgements**

427 This study was funded by a European Research Council Starting Grant (ELEVATE:
428 ERC-2017-STG-757810) to JZS. Benjamin Conlon assisted with statistical analyses. Useful
429 comments were provided by Jacobus Boomsma, Gareth W. Griffith and Pedro Elias
430 Marques. The images recreating stages of gongylidium formation in Figure 4 were
431 produced by Damond Kyllo. Assistance with transmission and scanning electron
432 microscopies was provided by the Core Facility for Integrated Microscopy, Faculty of

433 Health and Medical Sciences, and the Zoological Museum, both at University of
434 Copenhagen. Data processing and analysis were performed using Computerome, the National
435 Life Science Supercomputer at DTU (www.computerome.dk). Sylvia Mathiasen and Rasmus
436 Larsen provided general laboratory assistance.

References

1. Solberg MF, Robertsen G, Sundt-Hansen LE, Hindar K, Glover KA. Domestication leads to increased predation susceptibility. Scientific Reports. 2020;10(1):1929.

2. Milla R, Osborne CP, Turcotte MM, Violle C. Plant domestication through an ecological lens. Trends Ecol Evol. 2015;30(8):463-9.

3. Gering E, Incorvaia D, Henriksen R, Conner J, Getty T, Wright D. Getting Back to Nature: Feralization in Animals and Plants. Trends Ecol Evol. 2019;34(12):1137-51.

4. Comai L. The advantages and disadvantages of being polyploid. Nature Reviews Genetics. 2005;6(11):836-46.

5. Stetter MG, Gates DJ, Mei W, Ross-Ibarra J. How to make a domesticate. Curr Biol. 2017;27(17):R896-R900.

6. Edger PP, Poorten TJ, VanBuren R, Hardigan MA, Colle M, McKain MR, et al. Origin and evolution of the octoploid strawberry genome. Nat Genet. 2019;51(3):541-7.

7. Piperno DR. Patterns, Process, and New Developments

The Origins of Plant Cultivation and Domestication in the New World Tropics. CurrAnthr. 2011;52(S4):S453-S70.

8. Renner SS, Wu S, Pérez-Escobar OA, Silber MV, Fei Z, Chomicki G. A chromosome-level genome of a Kordofan melon illuminates the origin of domesticated watermelons. Proc Natl Acad Sci. 2021;118(23):e2101486118.

9. Mueller UG, Gerardo NM, Aanen DK, Six DL, Schultz TR. The evolution of agriculture in insects. Annual Review of Ecology, Evolution, and Systematics. 2005:563-95.

10. Schultz TR, Brady SG. Major evolutionary transitions in ant agriculture. Proc Natl Acad Sci. 2008;105(14):5435-40.

11. Barrera CA, Sosa-Calvo J, Schultz TR, Rabeling C, Bacci Jr M. Phylogenomic reconstruction reveals new insights into the evolution and biogeography of Atta leaf-cutting ants (Hymenoptera: Formicidae). Syst Entomol. 2021;n/a(n/a).

12. Boomsma JJ. Lifetime Commitment between Social Insect Families and Their Fungal Cultivars Complicates Comparisons with Human Farming. In: Schultz TR, Gawne R, Peregrine PN, editors. The Convergent Evolution of Agriculture in Humans and Insects. Vienna Series in Theoretical Biology. Cambridge, Massachusetts: MIT Press; 2022. p. 73-86.

13. Frank SA. Host-symbiont conflict over the mixing of symbiotic lineages. Proceedings of the Royal Society of London Series B: Biological Sciences. 1996;263(1368):339-44.

14. Axelrod R, Hamilton WD. The Evolution of Cooperation. Science. 1981;211(4489):1390-6.

15. Boomsma JJ, Gawne R. Superorganismality and caste differentiation as points of no return: how the major evolutionary transitions were lost in translation. Biological Reviews. 2018;93(1):28-54.

16. Leigh Jr EG. The evolution of mutualism. J Evol Biol. 2010;23(12):2507-28.

17. Hölldobler B, Wilson EO. The leafcutter ants: civilization by instinct. New York: W. W Norton & Co.; 2011.

18. Wirth R, Herz H, Ryel RJ, Beyschlag W, Hölldobler B. Herbivory of Leaf-Cutting Ants. Germany: Springer-Verlag Berlin Heidelberg; 2003. 233 p.

19. Crumiere AJJ, James A, Lannes P, Mallett S, Michelsen A, Rinnan R, et al. The multidimensional nutritional niche of fungus-cultivar provisioning in free-ranging colonies of a neotropical leafcutter ant. Ecol Lett. 2021;24(11):2439-51.

20. Mueller UG, Schultz TR, Currie CR, Adams RM, Malloch D. The origin of the attine ant-fungus mutualism. Q Rev Biol. 2001:169-97.

21. Quinlan RJ, Cherrett JM. The role of fungus in the diet of the leaf-cutting ant Atta cephalotes (L.). Ecol Entomol. 1979;4(2):151-60.

22. Weber NA. Dry season adaptations of fungus-growing ants and their fungi. The Anatomical Record. 1957;128(3):1.

23. Wheeler WM. The fungus-growing ants of North America. Bulletin of the American Museum of Natural History. 1907;23:139.

24. Möller A. Die Pilzgärten einiger südamerikanischer Ameisen. A.F.W. S, editor. Jena: Gustav Fischer Verlag; 1893.

25. Powell RJ. The influence of substrate quality on fungus cultivation by some Attine ants: University of Exeter; 1984.

26. Weber NA. Fungus-growing ants. Science. 1966;153(3736):587-604.

27. Swingle WT. Fungus Gardens in the Nest of an Ant (Atta tardigrada Buckl.) near Washington. Proc Am Assoc Adv Sci. 1896;44th Meet.:2.

28. Nygaard S, Hu H, Li C, Schiøtt M, Chen Z, Yang Z, et al. Reciprocal genomic evolution in the ant–fungus agricultural symbiosis. Nat Commun. 2016;7:12233.

29. Solomon SE, Rabeling C, Sosa-Calvo J, Lopes CT, Rodrigues A, Vasconcelos HL, et al. The molecular phylogenetics of Trachymyrmex Forel ants and their fungal cultivars provide insights into the origin and coevolutionary history of 'higher-attine' ant agriculture. Syst Entomol. 2019;44(4):939-56.

30. De Fine Licht HH, Schiøtt M, Rogowska-Wrzesinska A, Nygaard S, Roepstorff P, Boomsma JJ. Laccase detoxification mediates the nutritional alliance between leaf-cutting ants and fungus-garden symbionts. Proc Natl Acad Sci. 2013;110(2):583-7.

31. Kooij PW, Rogowska-Wrzesinska A, Hoffmann D, Roepstorff P, Boomsma JJ, Schiott M. *Leucoagaricus gongylophorus* uses leaf-cutting ants to vector proteolytic enzymes towards new plant substrate. ISME J. 2014;8(5):1032-40.

32. Schiøtt M, Rogowska-Wrzesinska A, Roepstorff P, Boomsma JJ. Leaf-cutting ant fungi produce cell wall degrading pectinase complexes reminiscent of phytopathogenic fungi. BMC Biol. 2010;8(1):156.

33. Aylward FO, Khadempour L, Tremmel DM, McDonald BR, Nicora CD, Wu S, et al. Enrichment and Broad Representation of Plant Biomass-Degrading Enzymes in the Specialized Hyphal Swellings of Leucoagaricus gongylophorus, the Fungal Symbiont of Leaf-Cutter Ants. PLOS ONE. 2015;10(8):e0134752.

34. Schiøtt M, Boomsma JJ. Proteomics reveals synergy between biomass degrading enzymes and inorganic Fenton chemistry in leaf-cutting ant colonies. eLife. 2021;10:e61816.

35. Martin MM. The Biochemical Basis of the Fungus-Attine Ant Symbiosis. Science. 1970;169(3940):16.

36. Martin MM, Martin JS. The biochemical basis for the symbiosis between the ant, Atta colombica tonsipes, and its food fungus. J Insect Physiol. 1970;16(1):109-19.

527 37. Khadempour L, Kyle JE, Webb-Robertson B-JM, Nicora CD, Smith FB, Smith
528 RD, et al. From Plants to Ants: Fungal Modification of Leaf Lipids for Nutrition and
529 Communication in the Leaf-Cutter Ant Fungal Garden Ecosystem. mSystems.
530 2021;6(2):e01307-20.

531 38. Shik JZ, Rytter W, Arnan X, Michelsen A. Disentangling nutritional pathways
532 linking leafcutter ants and their co-evolved fungal symbionts using stable isotopes.
533 Ecology. 2018;99(9):1999-2009.

534 39. Martin MM, Carman RM, MacConnell JG. Nutrients Derived from the Fungus
535 Cultured by the Fungus-Growing Ant Atta colombica tonsipes1. Ann Entomol Soc Am.
536 1969;62(1):11-3.

537 40. De Fine Licht HH, Boomsma JJ, Tunlid A. Symbiotic adaptations in the fungal
538 cultivar of leaf-cutting ants. Nat Commun. 2014;5(1):5675.

539 41. Kikuma T, Ohneda M, Arioka M, Kitamoto K. Functional Analysis of the *ATG8*
540 Homologue Ao*atg8* and Role of Autophagy in Differentiation and Germination in
541 *Aspergillus oryzae*. Eukaryot Cell. 2006;5(8):1328-36.

542 42. Pinan-Lucarré B, Paoletti M, Dementhon K, Coulary-Salin B, Clavé C.
543 Autophagy is induced during cell death by incompatibility and is essential for
544 differentiation in the filamentous fungus Podospora anserina. Mol Microbiol.
545 2003;47(2):321-33.

546 43. Liu X-H, Gao H-M, Xu F, Lu J-P, Devenish RJ, Lin F-C. Autophagy vitalizes the
547 pathogenicity of pathogenic fungi. Autophagy. 2012;8(10):1415-25.

548 44. Kües U, Navarro-González M. How do Agaricomycetes shape their fruiting
549 bodies? 1. Morphological aspects of development. Fungal Biology Reviews.
550 2015;29(2):63-97.

551 45. Elander PH, Minina EA, Bozhkov PV. Autophagy in turnover of lipid stores:
552 trans-kingdom comparison. J Exp Bot. 2017;69(6):1301-11.

553 46. Bartoszewska M, Kiel JA. The role of macroautophagy in development of
554 filamentous fungi. Antioxid Redox Signal. 2011;14(11):2271-87.

555 47. Levine B, Klionsky DJ. Development by Self-Digestion: Molecular Mechanisms
556 and Biological Functions of Autophagy. Dev Cell. 2004;6(4):463-77.

557 48. Klionsky DJ, Abdel-Aziz AK, Abdelfatah S, Abdellatif M, Abdoli A, Abel S, et al.
558 Guidelines for the use and interpretation of assays for monitoring autophagy (4th
559 edition)1. Autophagy. 2021;17(1):1-382.

560 49. Angeli-Papa J, Eymé J. Le champignon cultivé par la" fourmi-manioc",
561 Acromyrmex octospinosus Reich en Guadeloupe; résultats préliminaires sur le
562 mycélium en culturue pure et sur l'infrastructure des hyphes. C r hebd Séanc Acad Sci,
563 Paris D 1979;281:21-4.

564 50. Noda T, Ohsumi Y. Tor, a Phosphatidylinositol Kinase Homologue, Controls
565 Autophagy in Yeast*. J Biol Chem. 1998;273(7):3963-6.

566 51. Mauthe M, Orhon I, Rocchi C, Zhou X, Luhr M, Hijlkema K-J, et al. Chloroquine
567 inhibits autophagic flux by decreasing autophagosome-lysosome fusion. Autophagy.
568 2018;14(8):1435-55.

569 52. Wu Y-T, Tan H-L, Shui G, Bauvy C, Huang Q, Wenk MR, et al. Dual Role of 3-
570 Methyladenine in Modulation of Autophagy via Different Temporal Patterns of Inhibition
571 on Class I and III Phosphoinositide 3-Kinase*. J Biol Chem. 2010;285(14):10850-61.

572 53. Shik JZ, Kooij PW, Donoso DA, Santos JC, Gomez EB, Franco M, et al.
573 Nutritional niches reveal fundamental domestication trade-offs in fungus-farming ants.
574 Nat Ecol Evol. 2021;5(1):122-34.

575 54. Schneider CA, Rasband WS, Eliceiri KW. NIH Image to ImageJ: 25 years of
576 image analysis. Nat Methods. 2012;9(7):671-5.

577 55. R Core Team. R: a language and environment for statistical computing.
578 Foundation for Statistical Computing. Vienna, Austria 2020.

579 56. Kassambara A. rstatix: Pipe-Friendly Framework for Basic Statistical Tests. R
580 package version 0.7.0. ed2021.

581 57. Grabherr MG, Haas BJ, Yassour M, Levin JZ, Thompson DA, Amit I, et al. Full-
582 length transcriptome assembly from RNA-Seq data without a reference genome. Nat
583 Biotechnol. 2011;29(7):644-52.

584 58. Fu L, Niu B, Zhu Z, Wu S, Li W. CD-HIT: accelerated for clustering the next-
585 generation sequencing data. Bioinformatics. 2012;28(23):3150-2.

586 59. Li B, Dewey CN. RSEM: accurate transcript quantification from RNA-Seq data
587 with or without a reference genome. BMC Bioinformatics. 2011;12(1):323.

588 60. Love MI, Huber W, Anders S. Moderated estimation of fold change and
589 dispersion for RNA-seq data with DESeq2. Genome Biology. 2014;15(12):550.

590 61. Kanehisa M, Goto S. KEGG: Kyoto Encyclopedia of Genes and Genomes.
591 Nucleic Acids Res. 2000;28(1):27-30.

592 62. Kanehisa M, Sato Y, Morishima K. BlastKOALA and GhostKOALA: KEGG
593 Tools for Functional Characterization of Genome and Metagenome Sequences. J Mol
594 Biol. 2016;428(4):726-31.

595 63. Aramaki T, Blanc-Mathieu R, Endo H, Ohkubo K, Kanehisa M, Goto S, et al.
596 KofamKOALA: KEGG Ortholog assignment based on profile HMM and adaptive score
597 threshold. Bioinformatics. 2019;36(7):2251-2.

598 64. Grell MN, Linde T, Nygaard S, Nielsen KL, Boomsma JJ, Lange L. The fungal
599 symbiont of *Acromyrmex* leaf-cutting ants expresses the full spectrum of genes to
600 degrade cellulose and other plant cell wall polysaccharides. BMC Genomics. 2013;14.

601 65. Mueller UG, Mikheyev AS, Hong E, Sen R, Warren DL, Solomon SE, et al.
602 Evolution of cold-tolerant fungal symbionts permits winter fungiculture by leafcutter ants
603 at the northern frontier of a tropical ant–fungus symbiosis. Proc Natl Acad Sci.
604 2011;108(10):4053-6.

605 66. Nichols-Orians CM. Environmentally Induced Differences in Plant Traits:
606 Consequences for Susceptibility to a Leaf-Cutter Ant. Ecology. 1991;72(5):1609-23.

607 67. Howard JJ. Leafcutting Ant Diet Selection: The Role of Nutrients, Water, and
608 Secondary Chemistry. Ecology. 1987;68(3):503-15.

609 68. Howard JJ. Leafcutting and Diet Selection: Relative Influence of Leaf Chemistry
610 and Physical Features. Ecology. 1988;69(1):250-60.

611 69. Nichols-Orians CM, Schultz JC. Interactions among leaf toughness, chemistry,
612 and harvesting by attine ants. Ecol Entomol. 1990;15(3):311-20.

613 70. Crumiere AJJ, Mallett S, Michelsen A, Rinnan R, Shik JZ. Nutritional challenges
614 of feeding a mutualist: Testing for a nutrient-toxin tradeoff in fungus-farming leafcutter
615 ants. Ecology. 2022;103(6):e3684.

71. Mundim FM, Costa AN, Vasconcelos HL. Leaf nutrient content and host plant selection by leaf-cutter ants, Atta laevigata, in a Neotropical savanna. Entomol Exp Appl. 2009;130(1):47-54.

72. Berish CW. Leaf-Cutting Ants (Atta cephalotes) Select Nitrogen-Rich Forage. The American Midland Naturalist. 1986;115(2):268-76.

73. Howard JJ, Cazin J, Wiemer DF. Toxicity of terpenoid deterrents to the leafcutting antAtta cephalotes and its mutualistic fungus. J Chem Ecol. 1988;14(1):59-69.

74. Jandér KC, Herre EA. Host sanctions and pollinator cheating in the fig tree-fig wasp mutualism. Proc R Soc B. 2010;277(1687):1481-8.

75. Heil M, McKey D. Protective Ant-Plant Interactions as Model Systems in Ecological and Evolutionary Research. Annual Review of Ecology, Evolution, and Systematics. 2003;34(1):425-553.

76. Kiers ET, Rousseau RA, West SA, Denison RF. Host sanctions and the legume–rhizobium mutualism. Nature. 2003;425(6953):78-81.

77. Bass M, Cherrett JM. Leaf-Cutting Ants (Formicidae, Attini) Prune Their Fungus to Increase and Direct Its Productivity. Funct Ecol. 1996;10(1):55-61.

78. Schiøtt M, De Fine Licht HH, Lange L, Boomsma JJ. Towards a molecular understanding of symbiont function: Identification of a fungal gene for the degradation of xylan in the fungus gardens of leaf-cutting ants. BMC Microbiol. 2008;8(1):40.

79. Moller IE, De Fine Licht HH, Harholt J, Willats WGT, Boomsma JJ. The Dynamics of Plant Cell-Wall Polysaccharide Decomposition in Leaf-Cutting Ant Fungus Gardens. PLOS ONE. 2011;6(3):e17506.

80. Nygaard S, Zhang G, Schiøtt M, Li C, Wurm Y, Hu H, et al. The genome of the leaf-cutting ant Acromyrmex echinatior suggests key adaptations to advanced social life and fungus farming. Genome Res. 2011;21(8):1339-48.

81. Shik JZ, Gomez EB, Kooij PW, Santos JC, Wcislo WT, Boomsma JJ. Nutrition mediates the expression of cultivar–farmer conflict in a fungus-growing ant. Proc Natl Acad Sci. 2016;113(36):10121-6.

82. Pinto-Tomás AA, Anderson MA, Suen G, Stevenson DM, Chu FST, Cleland WW, et al. Symbiotic Nitrogen Fixation in the Fungus Gardens of Leaf-Cutter Ants. Science. 2009;326(5956):1120-3.

83. Khadempour L, Fan H, Keefover-Ring K, Carlos-Shanley C, Nagamoto NS, Dam MA, et al. Metagenomics Reveals Diet-Specific Specialization of Bacterial Communities in Fungus Gardens of Grass- and Dicot-Cutter Ants. Frontiers in Microbiology. 2020;11.

84. Sapountzis P, Zhukova M, Shik JZ, Schiott M, Boomsma JJ. Reconstructing the functions of endosymbiotic Mollicutes in fungus-growing ants. eLife. 2018;7:e39209.

85. Zhukova M, Sapountzis P, Schiøtt M, Boomsma J. Phylogenomic analysis and metabolic role reconstruction of mutualistic Rhizobiales hindgut symbionts of *Acromyrmex* leaf-cutting ants. FEMS Microbiol Ecol. In press.

86. Kooij PW, Aanen DK, Schiøtt M, Boomsma JJ. Evolutionarily advanced ant farmers rear polyploid fungal crops. J Evol Biol. 2015;28(11):1911-24.

87. Xiang X, Beckwith SM, Morris NR. Cytoplasmic dynein is involved in nuclear migration in Aspergillus nidulans. Proc Natl Acad Sci. 1994;91(6):2100-4.

88. Xiang X. Nuclear movement in fungi. Semin Cell Dev Biol. 2018;82:3-16.

662 89. Yamamoto A, Hiraoka Y. Cytoplasmic dynein in fungi: insights from nuclear
663 migration. J Cell Sci. 2003;116(22):4501-12.

664 90. Plamann M, Minke PF, Tinsley JH, Bruno KS. Cytoplasmic dynein and actin-
665 related protein Arp1 are required for normal nuclear distribution in filamentous fungi. J
666 Cell Biol. 1994;127(1):139-49.

667 91. Gehrmann T, Pelkmans JF, Ohm RA, Vos AM, Sonnenberg ASM, Baars JJP, et
668 al. Nucleus-specific expression in the multinuclear mushroom-forming fungus *Agaricus*
669 *bisporus* reveals different nuclear regulatory programs. Proc Natl Acad Sci U S A.
670 2018;115(17):4429-34.

671 92. Stalpers JA. Identification of wood-inhabiting Aphyllophorales in pure culture.
672 Studies in Mycology. 1978;16:248.

673 93. Nobles MK. Identification of cultures of wood-inhabiting Hymenomycetes.
674 Canadian Journal of Botany. 1965;43(9):1097-139.

675

676 **Figures and table**

677

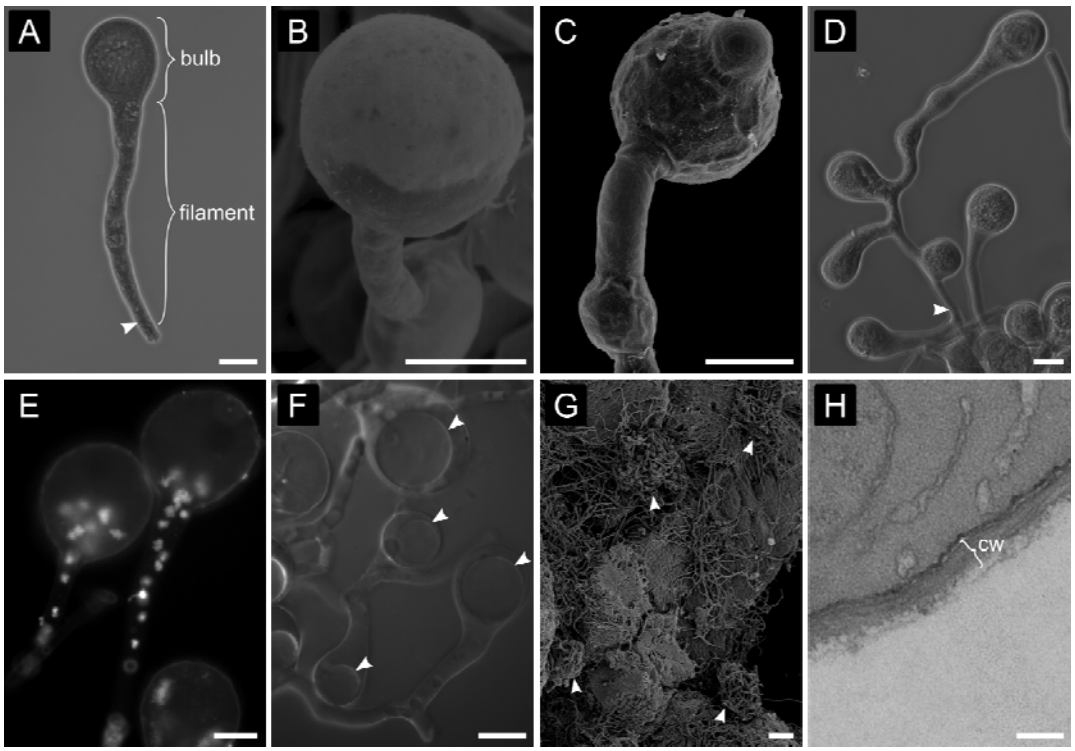

678

679 **Fig. 1: The *Leucoagaricus gongylophorus* fungal cultivar produces gongylidia as**
680 **specialized nutritional reward structures for leafcutter ants. A-C)** Gongylidium cells are
681 typically depicted as a bulb at the end of a filament in the apical hyphal compartment separated
682 by a septum (arrowheads). **D)** Gongylidia frequently exhibit more complex branching, with bulbs
683 between filaments or in lateral branches of single hyphal cells delimited by septa. **E)** Individual
684 gongylidium cells are polykaryotic [86], meaning that they have many haploid nuclei (white
685 dots). Here, we show that in mature non-branching gongylidium cells, these nuclei occur at the
686 base of the bulb (below a single large vacuole) and in the filament. Nuclei were visualized using
687 DAPI staining. **F)** Each gongylidium cell contains a large vacuole (arrowheads). **G)** Staphyla
688 grow in discrete patches at the surface of the fungus garden matrix in the middle garden
689 stratum (arrowheads). **H)** Gongylidium cells have thin cell walls ranging from 120 to 220 nm
690 (cw). Images produced by light microscopy (panels A, D, F), fluorescence microscopy stained
691 with DAPI (panel E), SEM (panels B, C, G) and TEM (panel H). Scale bars: A-F = 20 µm, G =
692 100 µm, H = 200 nm.

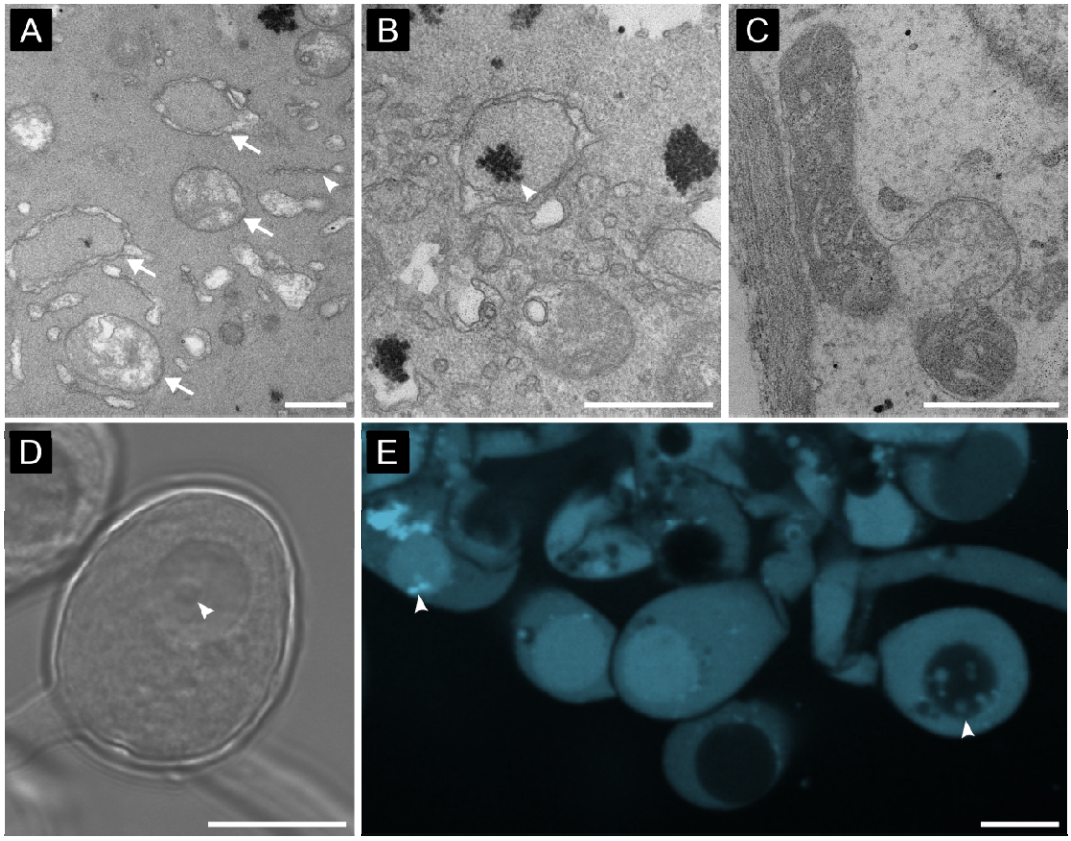

693

694 **Fig. 2: Autophagic recycling of cellular material. A)** The autophagosomes that are diagnostic
695 of autophagy are vesicles with double-layered membranes (arrows) and are produced by
696 stretches of endoplasmic reticulum membranes (arrowheads). **B)** Autophagosomes sequester
697 cytoplasmic components including glycogen (arrowhead) and **C)** mitochondria which are then
698 delivered to vacuoles in gongylidia bulbs for further degradation. **D-E)** Vacuolar expansion is
699 mediated by autophagosomes that lose their outer membrane after fusing with the vacuole.
700 These single-membraned autophagic bodies are vesicles that can be seen inside the vacuole
701 prior to their degradation (arrowhead). Images acquired by TEM (A-C), phase contrast
702 microscopy (D) and confocal microscopy stained with dextran-Alexa fluor 647 (E). Scale bars A-
703 C = 500 nm, D-E = 20 µm.

704

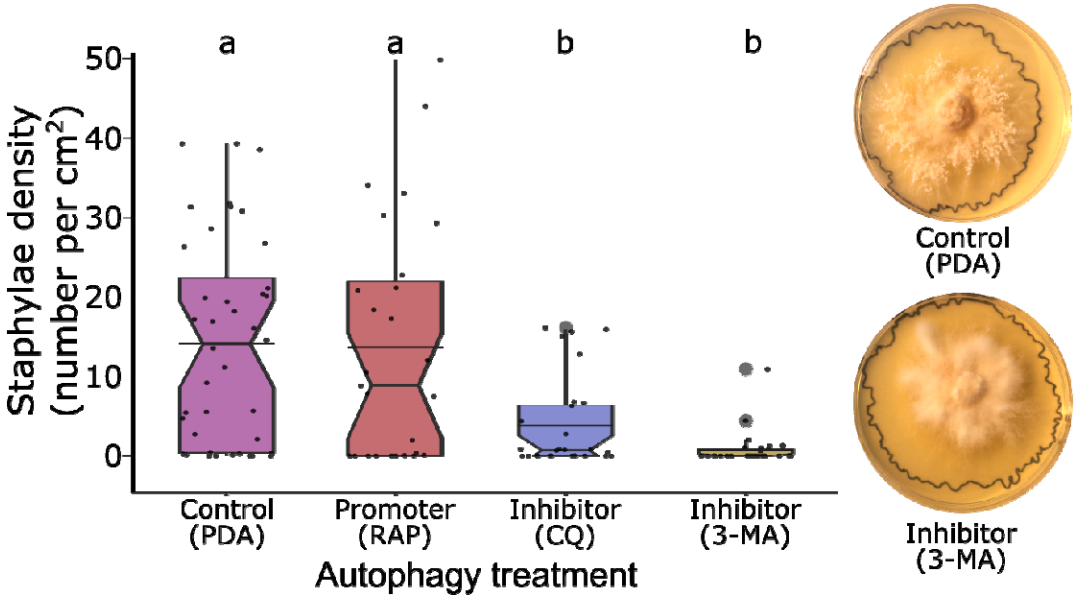

705

706 **Fig. 3: Experimental evidence that autophagic recycling of the fungal cultivar's own**
707 **cellular material mediates gongylidia formation.** Gongylidium density was significantly
708 inhibited when *L. gongylophorus* was grown on potato dextrose agar supplemented with one
709 autophagy inhibitor chloroquine (CQ, n = 28) or 3-methyladenine (3-MA, n = 30)) relative to
710 control (PDA, n = 40) and an autophagy promoter rapamycin (RAP, n = 27)). Representative
711 Petri-dishes with control (PDA; top) and inhibition (CQ; bottom) are displayed at the right, black
712 outlines indicate the radial growth area of cultivars and white fungal clusters in the control are
713 the staphylae. Different letters above the boxes indicate significant differences determined by a
714 post-hoc Dunn's pairwise test ($p < 0.05$) and horizontal bars indicate the distribution means.

715

716

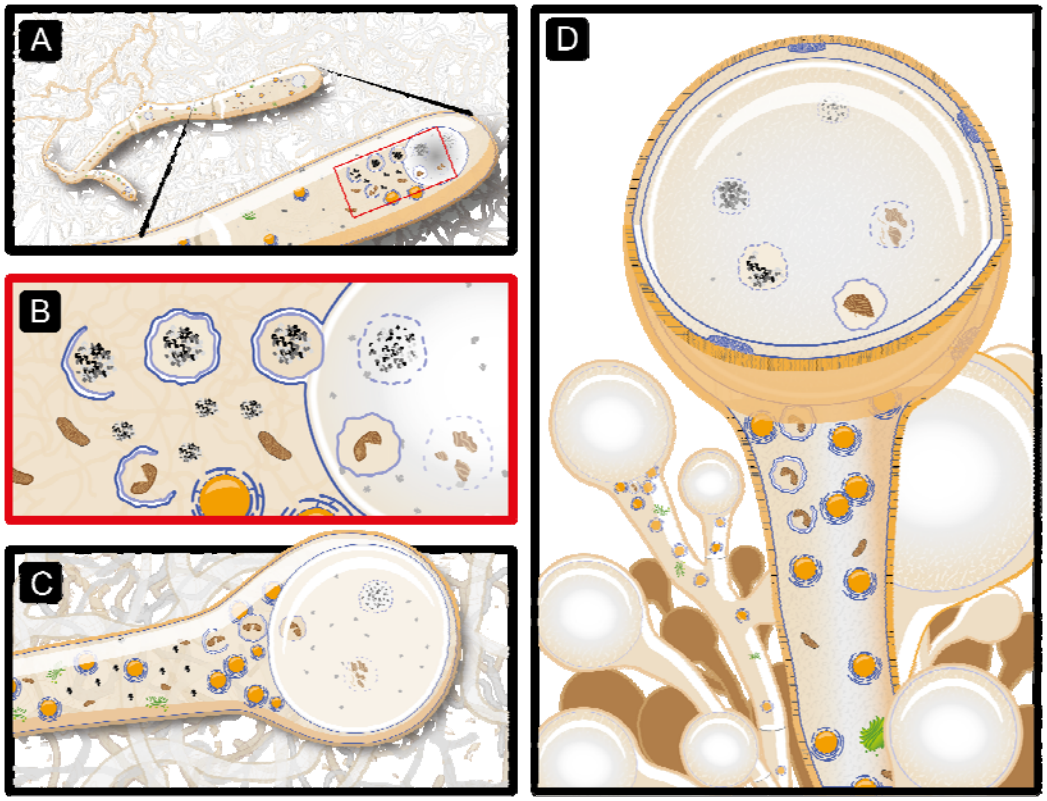

717

718 **Fig. 4: The hypothesized stages of autophagy-mediated gongylidium development. A)** An
719 unknown mechanism (potentially starvation mediated by ant pruning [77]) triggers the widening
720 of ordinary hyphae. As the hypha elongates, the nuclei (orange circles) naturally migrate
721 towards the hyphal tip. **B)** Mediated primarily by an autophagic process, a large vacuole
722 expands with the fusion of newly formed double membrane vesicles called autophagosomes
723 (blue membraned vesicles) that sequester material present in the cytosol like glycogen (black
724 and gray aggregates) and damaged mitochondria (brown indented ovals). This process is
725 indicated by the proliferation of endoplasmic reticulum membranes (blue membranes around
726 nuclei) that produce autophagosomes. **C)** The fusion of autophagosomes into vacuoles
727 mediates their expansion and either forces the apical bulb swelling while also halting further
728 apical growth by excluding nuclei from the hyphal tip or produce an intercalary bulb when the
729 vacuole is located among nuclei. **D)** This process repeats in up to hundreds of adjacent hyphae
730 that become tangled to form the staphyla.

731

732 **Table 1:** Upregulated transcripts in autophagy pathway annotated with KEGG database (see Fig. S3).

Tissue	KEGG	Gene names	No. of transcripts
Staphylae	K06902	ATG22; UMF1; MFS transporter, UMF1 family	1
	K07897	Ypt7; RAB7A; Ras-related protein Rab-7A	1
	K08331	ATG13; autophagy-related protein 13	1
	K08337	ATG7; ubiquitin-like modifier-activating enzyme ATG7	3
	K12767	RIM15; serine/threonine-protein kinase RIM15	2
	K17606	IGBP1, TAP42; immunoglobulin-binding protein 1	1
	K17888	ATG10; ubiquitin-like-conjugating enzyme ATG10	1
	K17900	ATG15, AUT5; lipase ATG15	1
	K01336	PRB1; cerevisin	5
	K08341	ATG8, GABARAP, LC3; GABA(A) receptor-associated protein	1
	K19800	SCH9; serine/threonine protein kinase SCH9	1
	K20177	VPS3, TGFBRAP1; vacuolar protein sorting-associated protein 3	2
	K20195	MON1; vacuolar fusion protein MON1	2
Mycelium	K01336	PRB1; cerevisin	1
	K04464	MAPK7; mitogen-activated protein kinase 7	2
	K08337	ATG7; ubiquitin-like modifier-activating enzyme ATG7	2
	K12761	SNF1; carbon catabolite-derepressing protein kinase	1
	K17906	ATG2; autophagy-related protein 2	1
	K21157	SAK1; SNF1-activating kinase 1	1
	K06655	PHO85; negative regulator of the PHO system	1

733
734

735 **Supplementary figures**

736

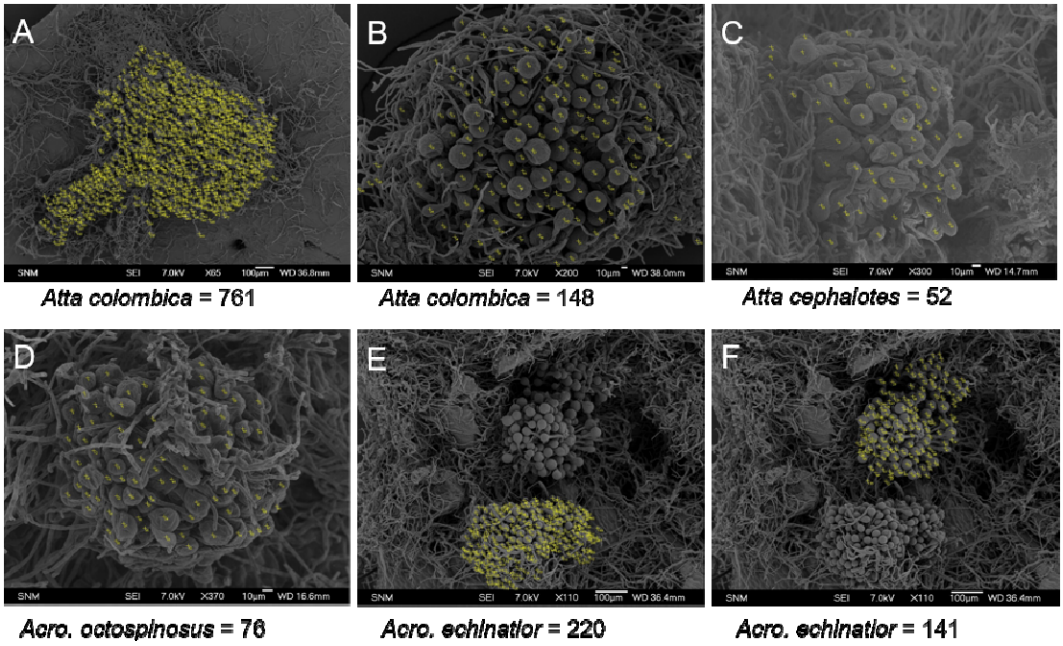

737

738 **Fig. S1: Representative counts of gongylidia per staphylae in *L. gongylophorus* from**
739 **different leafcutter ants' species.** A) Staphylae from in vitro culture without ant manipulation.
740 B-E) staphylae from colonies fungus garden. Yellow marks indicate individual gongylidia count
741 on ImageJ. Scale bars sizes are indicated in each image.

742

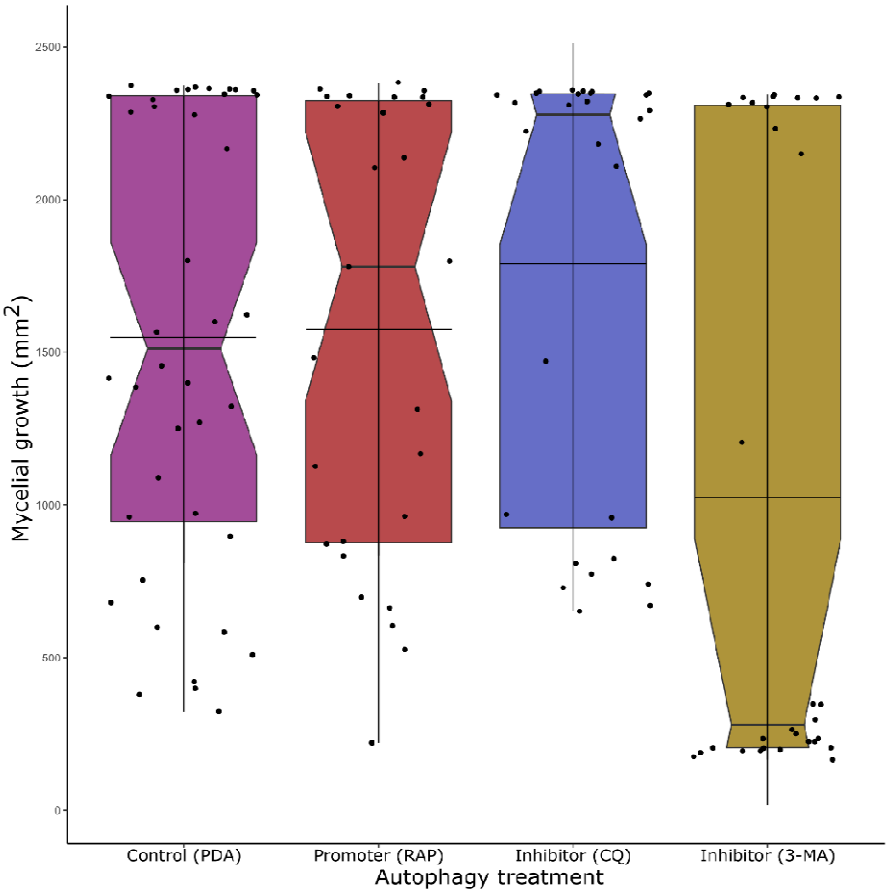

743

744 **Fig. S2: Mycelial growth distribution (area per treatment).** The mycelial growth showed
745 significant differences between 3-MA and all other treatments (PDA:3-MA, p_{adj} = 0.004; RAP:3-
746 MA, p_{adj} = 0.015; CQ:3-MA, p_{adj} = 0.001), but no other significant pairwise comparisons. Thus,
747 while both autophagy inhibition treatments resulted in staphyla reduction, it is possible that 3-
748 MA negatively influenced staphyla density through unknown indirect effects on cultivar
749 performance. Horizontal bars indicate the distribution means.

750

751

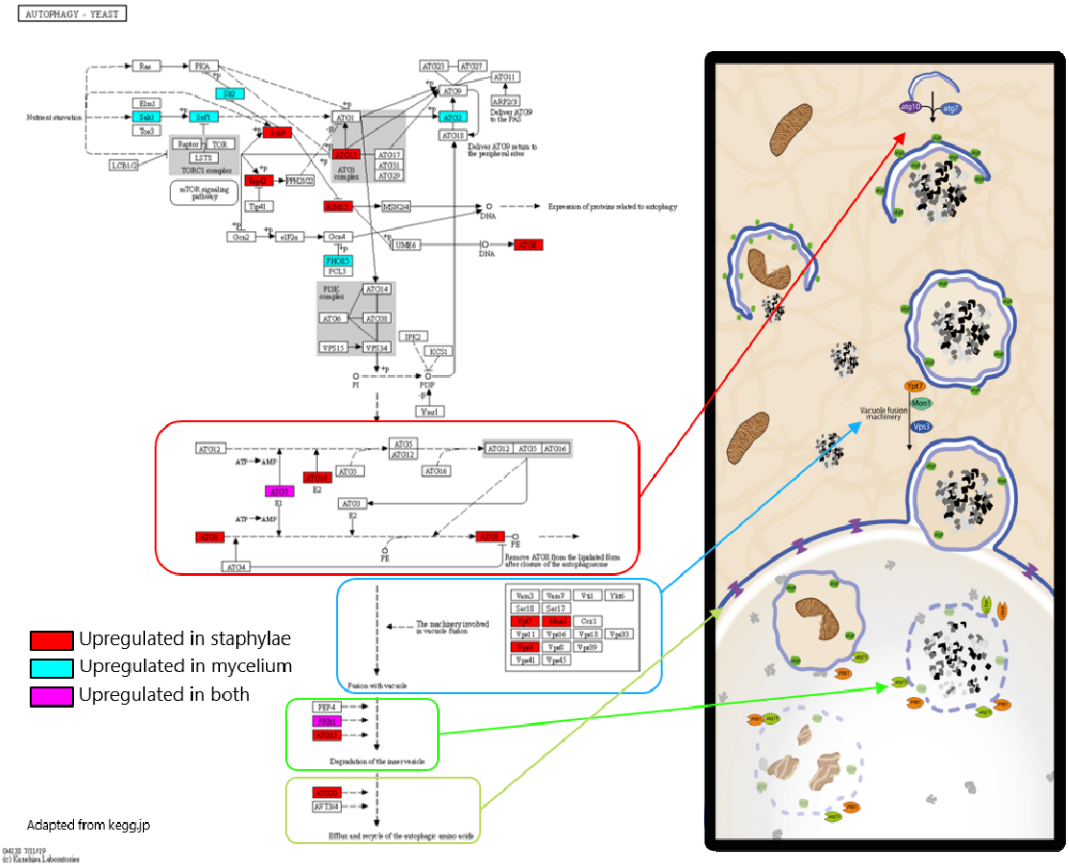

Fig. S3: Autophagy metabolic pathway map displaying gene expression in *L. gongylophorus*. Highlighted genes show upregulated transcripts in staphylae (red), mycelium (cyan) or in both tissues (magenta). The steps of the pathway are illustrated on the right showing where the products of these genes will act during autophagy. Adapted from KEGG website (www.kegg.jp).

Video S1: Time lapse of staphyla stained with dextran-Alexa Fluor 647 under confocal microscope over 20 minutes. Red arrows point gongylidia in which is possible to observe autophagic bodies trapped within the vacuole. Some of these vesicles are filled with dextran and appear more fluorescent than the vacuole lumen, others are filled with non-fluorescent material and appear darker than the vacuole.